Boundary Layer Transition on the Suction Side of a Turbine Blade

MARINA UBALDI, PIETRO ZUNINO
Department of Fluid Machines, Energy Systems and Transportation
University of Genova
Via Montallegro 1, I-16145 Genova
ITALY

Abstract: - Extensive measurements of velocity and turbulence have been performed by means of a two-component fibre-optic laser Doppler velocimeter, to investigate the profile boundary layer development on a large scale turbine cascade. Flow field investigation has been integrated with data obtained from surface-mounted hot-film gauges to get direct information on boundary layer nature and time varying characteristics. Measurements were detailed enough to allow constructing mean velocity and Reynolds stress boundary layer profiles giving an in-depth description of the boundary layer development through laminar, transitional and turbulent regimes.

Key-Words: - Axial flow turbines, Blade boundary layer, Transition, Laser Doppler measurements, Hot-film measurements.

1 Introduction

Accurate numerical prediction of the transitional boundary layer on turbomachinery blades is still a not completely resolved issue. Location and extension of transition has a large impact on loss production in turbine blades: for instance a too early transition can provoke a too large turbulent extension or a too late transition may not avoid laminar separation. Detailed experimental data specially produced for turbulence model assessment purpose, such as Reynolds stress and turbulence production term distributions, are of primary importance for improving the predictive capabilities of the transition models.

Results of a previous experimental investigation carried out on the same cascade at a larger Reynolds number [1] were extensively utilized by research groups operating in transition modeling [e.g. 2-4].

In the present study efforts have been made to obtain a comprehensive description of boundary layer mean velocity and Reynolds stress development on the suction side of a turbine blade, including laminar and transition regions. Most of the investigation was carried out by fibre-optic laser Doppler velocimeter. Direct information on the boundary layer condition was provided by analysing the fluctuating signals from surface-mounted hot-film gauges.

2 Test Facility and Test Conditions

The profile boundary layer development was surveyed on the blade suction side of a large-scale linear turbine cascade installed in the low-speed wind tunnel of the Aerodynamics and Turbomachinery Laboratory of the Department of Fluid Machines, Energy Systems and Transportation. The facility is a continuously operating variable speed wind tunnel with an open test section of 500x300 mm^2. A three-blade cascade with the largest possible blade chord was used so as to maximise measurement spatial resolution.

The blade profile is representative of a coolable hp gas turbine nozzle blade and is the same tested during an European project on time-varying wake flow characteristics on flat plates and turbine cascades [5]. The relevant geometrical characteristics of the cascade are: chord length c = 300 mm, pitch-to-chord ratio g/c = 0.7, blade aspect ratio h/c = 1, gauging angle β_2' = 19.2°.

During the experiment the cascade was operated at a Reynolds number based on the outlet flow conditions and chord length Re_{2c} of 590000. The upstream turbulence level was 3.0 %. The integral length scale evaluated from the power density spectrum of the streamwise velocity [6] was 3.7% of the cascade chord length.

3 Instrumentation

3.1 LDV instrumentation

A two-colour fibre optic LDV system with backscatter collection optics (Dantec Fiber Flow) was used for the present investigation. The light

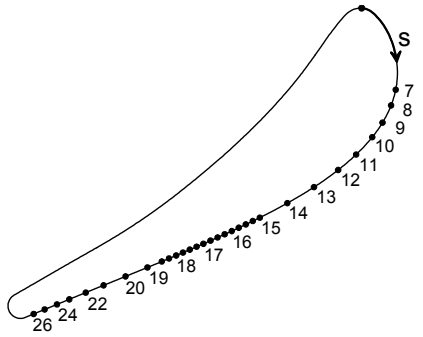

Fig. 1. Blade profile and measuring positions

source is a 300 mW argon ion laser operating at 488 nm (blue) and 514.5 nm (green).

The probe consists of an optical transducer head of 60 mm diameter connected to the emitting optics and to the photomultipliers by means of optic fibres. The probe volume of 47 μm diameter and 0.4 mm length contains two sets of blue and green fringes, which allow the simultaneous measurement of two velocity components in the plane perpendicular to the probe optical axis. A Bragg cell is used to apply a frequency shift (40 MHz) to one of each pair of beams, providing directional sensitivity and reducing angle bias for all velocity measurements. The signals from the photomultipliers are processed by two Enhanced Burst Spectrum Analysers.

3.2 Surface hot-film sensors

The single-sensor hot-film element (Dantec 55R47) consists of a 0.1x0.9 mm thin nickel film applied by vapour deposition on a 50 μm thick polyimide substrate.

Due to analogy between heat and momentum transfer in boundary layers, the local instantaneous wall shear stress is related to the rate of heat transfer from the hot sensor to the fluid [7]:

$$\tau_w = k\left[\left(e^2 - A^2\right)/\Delta T\right]^3 \qquad (1)$$

where e is the instantaneous voltage and ΔT is the temperature difference between sensor and fluid. As pointed out by several authors [8, 9], useful information on the transition and separation phenomena, as well as on boundary layer unsteady properties, can be obtained by a semi-quantitative analysis avoiding probe calibration. According to [10], eq. (1) can be approximated by

$$\tau_w \equiv k\left[\left(e^2 - e_0^{\,2}\right)/e_0^{\,2}\right]^3 \qquad (2)$$

where e_0 is the hot-film voltage at zero flow condition.

The quantity $\left[\left(e^2 - e_0^{\,2}\right)/e_0^{\,2}\right]^3$ is referred as instantaneous quasi wall shear stress $q\tau_w$.

4 Plan of Experiments

4.1 LDV measurements

The boundary layer was surveyed by means of 31 traverses normal to the blade surface at midspan. The location of the boundary layer traverses are shown in Fig. 1. Each boundary layer traverse is constituted by 34 measuring points. The distance between adjacent points was set at 25 μm in the region of the boundary layer close to the wall and was progressively increased in the outer part.

The measurements of the two velocity components were made in coincidence mode. Typical data rate was 10 kHz falling off to few kHz in the inner part of the boundary layer. For each measuring point 30000 samples were collected to obtain accurate statistical analysis. LDV data processing procedures are described in detail in [11].

4.2 Hot-film measurements

The gauge was glued on a 25 μm thick strip of acetate of length appropriate to avoid any surface discontinuity near the sensor. The strip was fixed on the blade surface by means of a thin bi-adhesive tape and easily repositioned to investigate the whole blade surface.

The film element was connected to a constant-temperature hot-wire unit (Dantec 55M10, 55M17), which maintains the film at the selected temperature difference with respect to the fluid (60 °C). The

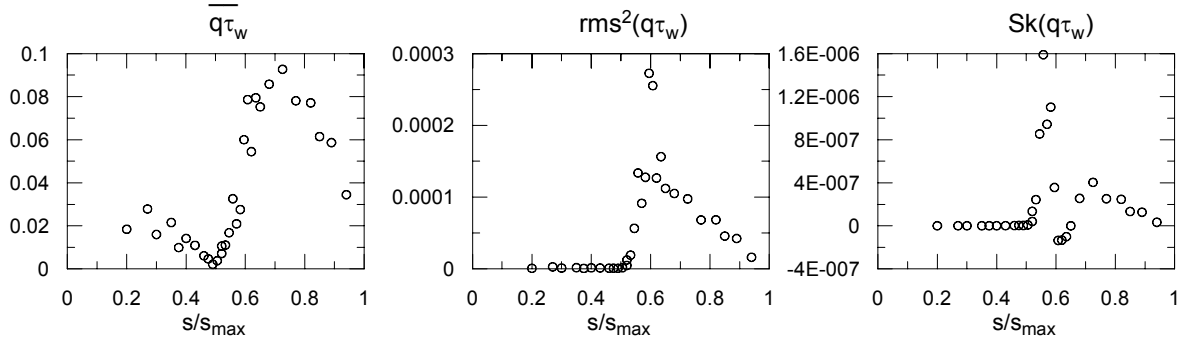

Fig. 2. Distributions of $q\tau_w$ statistical moments

system frequency response, deduced by a square wave test, exceeds 20 kHz. An antialiasing low-pass filter with a cut-off frequency of 20 kHz was applied to the anemometer signal before it was sampled at a frequency of 50 kHz by means of a 12 bit A/D converter board. For each measuring position a total of 172032 data was taken.

5 Analysis of the results

5.1 Surface hot-film results

Hot-films direct information from the wall are a very sensitive marker of the transition process. Statistical moments (average, variance and skewness coefficient) were evaluated and are here discussed to determine the boundary layer transition conditions.

Characteristic phases of the transition process can be clearly identified in Fig. 2. The start of the transition can be located at the position where the variance starts to increase and skewness moves from zero to positive values. This point is in the region

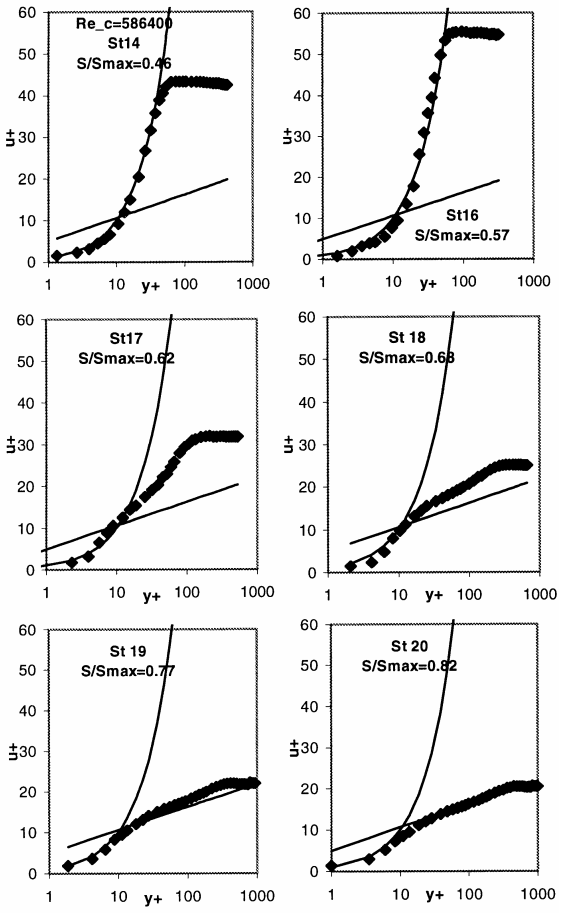

Fig. 3. Boundary layer mean velocity profiles in inner-law variables

where $\overline{q\tau_w}$ is attaining its relative minimum. The transition point can be defined by the maximum of the variance distribution, which corresponds to a region of large positive gradient of $\overline{q\tau_w}$ and to the position where the skewness coefficient is changing sign decreasing from the positive region to the negative one. Finally end of transition can be identified by the variance return to a nearly constant value and the skewness return to zero.

In the present results $\overline{q\tau_w}$ displays a clear relative minimum, which attains the null value at $s/s_{\max}$=0.5 exactly where variance moves steeply from zero and skewness becomes suddenly positive. Possibly this is a very special condition where both laminar separation and transition conditions occur at the same time.

5.2 LDV results

In order to get insight into the boundary layer transition process LDV instantaneous data are processed at three different levels:

- statistical moments and probability density functions;
- time traces of the instantaneous velocity and power density spectra;
- boundary layer integral parameters.

5.2.1 Statistical moments

Velocity and turbulence profiles are the most classical means of boundary layer analysis. In order to avoid statistical bias in the evaluation of the statistical moments for highly turbulent flows, transit time weighted averages have been applied to the LDV realizations [11].

Since in the inner region the boundary layer is governed by viscous effects, inner layer variables $u^+ = \overline{u}/u_\tau$ and $y^+ = yu_\tau/\nu$ are the most suitable coordinates for a careful evaluation of velocity and turbulence profiles.

Velocity profiles can be compared with well established semi-empirical correlations for turbulent boundary layers (e.g. White [12]):

- the linear correlation in the viscous sublayer range ($y^+ \le 5$): $u^+ = y^+$;
- the law of the wall in the overlap layer range $35 \le y^+ \le 350$: $u^+ = \frac{1}{k}\ln y^+ + B$

with k = 0.41 and B = 5.

Data fitting against analytical relationships allows to evaluate possible errors in wall location, to calculate wall friction velocity, and to identify if the boundary layer at that station is in laminar, turbulent

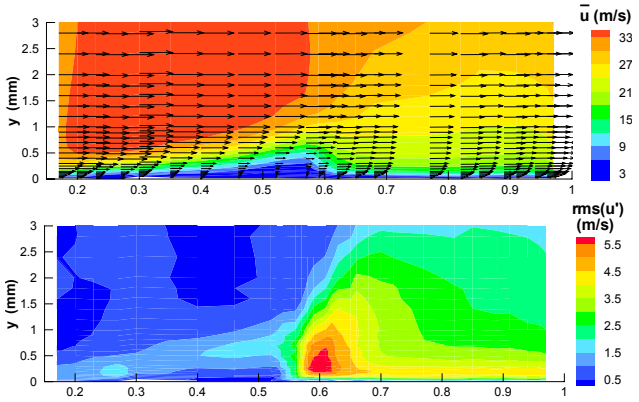

Fig. 4. Boundary layer velocity and turbulence

or transitional regime. An example of mean velocity profiles, showing the boundary layer development from laminar to turbulent through transitional conditions, is given in Fig. 3. Velocity profiles are laminar like until station 16, where the experimental data fit a large portion of the curve $u^+ = y^+$, they are transitional at station 17 and 18 and evolve to fully turbulent log-law profiles from station 19.

Thanks to the high spatial resolution of measurements, detailed colour plots of the statistical moments can be constructed, which provide an overall overview of the boundary layer development though the transition condition (Fig. 4). Transition may be easily detected by the steep and sudden increase of the standard deviation of the streamwise velocity fluctuations.

5.2.2 Velocity time traces and power spectra

Insight into the dynamic properties of the boundary layer transition can be obtained by the analysis of time traces of the instantaneous velocity and the associated power spectral density.

A measure of LDV capability in following the flow-velocity time-variations is given by the mean data density N_D, defined as the ratio between the integral time scale T_l and the mean valid data interarrival time Δt_S. The integral time scale T_l represents the period of the fluctuations associated with the largest flow structures.

Values of N_D of the order of 50 or larger are sufficient to provide a signal looking like a continuous representation of the velocity time history which allows a detailed description of the fine structure of the flow [13]. In the present investigation, the maximum obtainable data density is of the order of 20, a value that is not sufficient for the identification of the smallest flow fluctuations, but is large enough to reveal the general features of the time structure of the flow.

As an example Fig. 5 compares the time-series of measuring points of station 16 (in the transition region) with those of the corresponding points, at approximately the same y^+, of station 19 (in the turbulent region).

The most striking feature of the velocity traces of station 16 is the presence of not so frequent one-side velocity fluctuations, which determines the intermittent switching of the velocity from laminar to turbulent conditions. At y^+= 4.6 time trace shows also some negative velocity values, indicating the tendency of the boundary layer to separate.

At station 19, the turbulence structure is characterised by higher frequency two-side large velocity fluctuations.

Power spectral density offers a means to evaluate the energy distribution across the frequency range characteristic of the flow time-varying structure.

Figure 6 compares the power spectra for points located approximately at the same non-dimensional distance from the wall ($y^+ \cong$ 4.5 and 11) in transitional and turbulent traverses (stations 16 and 19, respectively).

The main difference between the two spectral distributions is the characteristic increase during transition of the spectral density in the low-frequency range (below 300 Hz), which is indicative of the broad band velocity fluctuations associated with the intermittent character of transition. For the turbulent condition, on the contrary, the spectral

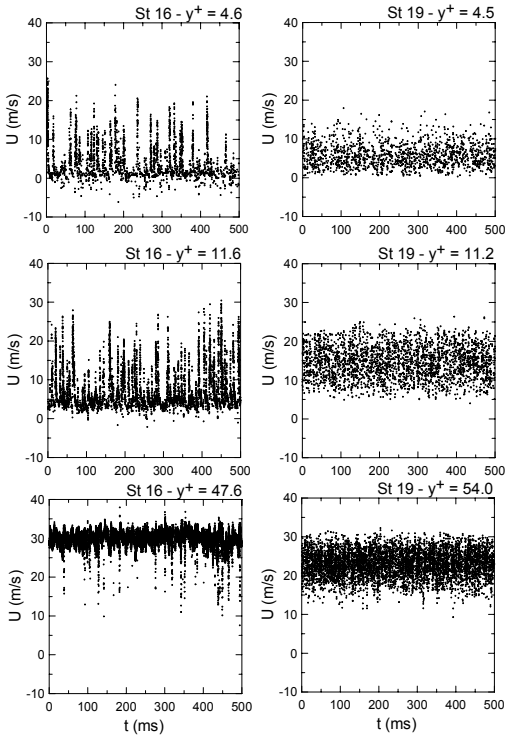

Fig. 5. Velocity time series

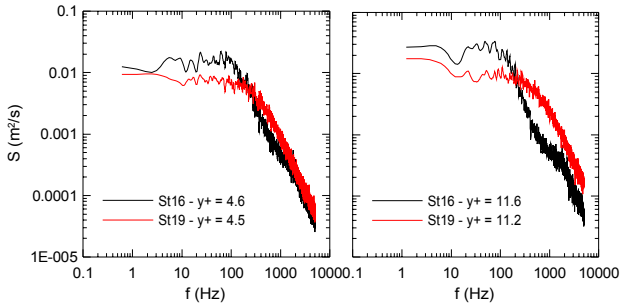

Fig. 6. Power density spectra

density increases in the higher frequency range.

5.2.3 Boundary layer integral parameters

Integral parameters provide global information essential for a practical evaluation of the boundary layer development such as flow blockage, energy losses and wall friction force. Integral parameter distributions are also sensitive indicators for identifying the boundary layer nature, the beginning and end of transition.

Integral parameters δ^* and ϑ have been evaluated by numerical integration of the experimental velocity profiles. Wall friction coefficient C_f, depending on u_τ / u_e, is evaluated in laminar and transitional regions by data fitting against the curve $u^+ = y^+$ in the linear sublayer and against the log-wall law in the turbulent region.

Integral parameters distributions of Fig. 7 indicate that the transition length is very short and the boundary layer remains in laminar state until $s/s_{max} = 0.55$. Before this position both δ^* and H_{12} show a characteristic steep increase, which indicates the tendency of the boundary layer to separation. At $s/s_{max} = 0.55$ suddenly both δ^* and H_{12} fall down towards turbulent values and within a portion of approximately 0.15 of the surface length, the transition is completed.

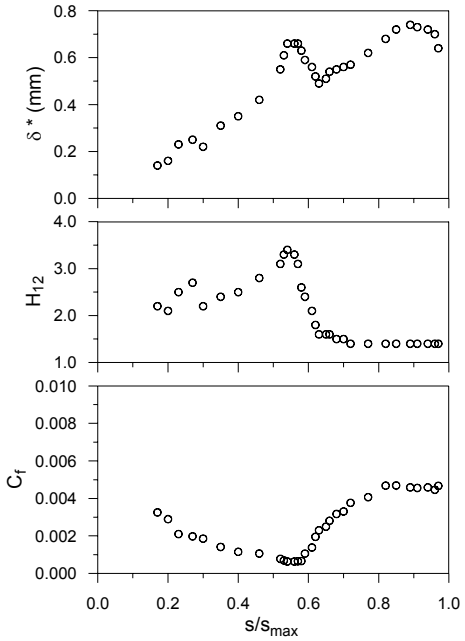

Fig. 7. Boundary layer integral parameters

From a practical standpoint the transition may be considered to begin where the skin friction coefficient deviates from the laminar values, showing a rapid increase. For the present experiments the C_f distributions substantially confirm the locations of start of transition previously identified by the hot-film measurements.

6 Conclusions

Results of an experimental investigation of the profile boundary layer in a large scale turbine cascade have been presented. Measurements have been performed by means of a two-component fibre-optic laser Doppler velocimeter. Direct information on the boundary layer nature has been achieved by means of surface-mounted hot-film sensors.

Thanks to the large scale of the cascade and the non-intrusive nature of LDV, a large amount of velocity data have been obtained in the near wall region. Data were used to construct profiles of mean velocity and Reynolds stress components, describing in detail the boundary layer development.

Boundary layer integral parameters provided overall engineering information useful for a practical evaluation of the boundary layer development.

LDV data rate was large enough to support the analysis of the dynamic properties of the transitional boundary layer.

The most relevant conclusions coming out from the present boundary layer study are the following.

- Both $q\tau_w$ and integral parameters distributions show that in the present experiment the transition starts suddenly at s/s_{max}=0.5, probably triggered by an incipient boundary layer separation, and it is rapidly completed at s/s_{max} =0.65.
- Velocity and turbulence profiles and contour plots document in detail the boundary layer development down to the near wall region. During transition the streamwise velocity fluctuations are strongly amplified especially in the near wall region and both u-rms and cross-correlation of velocity fluctuations attain values which are much larger than in the turbulent regime.
- Time traces of the instantaneous velocity taken at different distance from the blade surface show clearly the intermittent switches of the velocity

from laminar to turbulent conditions taking place in the near wall regions and the tendency of the boundary layer to separate before transition.

- Power spectral distributions show that during transition there is an energy increase in low-frequency range, which is indicative of the broad band velocity fluctuations due to the intermittent switches between laminar and turbulent states.

Accuracy and spatial resolution of measurements, and completeness of results make the present data a test case suitable for turbulence and transition models used in numerical prediction of boundary layer transition.

Nomenclature

C_f	wall friction coefficient $= 2\tau_w/(\rho u_e^2)$
f	frequency
H_{12}	shape factor = δ^*/θ
$q\tau_w$	quasi wall shear stress
S	spectral density
Sk	skewness coefficient
s	surface distance from leading edge
$s_{\max}$	surface length from leading to trailing edge
t	time
u, v	instantaneous velocity components in streamwise and cross-stream directions
u', v'	velocity fluctuations in streamwise and cross-stream directions
u_e	local free-stream velocity
u_τ	wall friction velocity = $\sqrt{\tau_w/\rho}$
u^+	dimensionless velocity = $\overline{u}/u_\tau$
y	normal distance from the blade surface
y^+	dimensionless distance $= yu_\tau/\nu$
δ^*	boundary layer displacement thickness
θ	boundary layer momentum thickness
ν	kinematic viscosity
ρ	fluid density
τ_w	wall shear stress

Overbar

— time averaged

References:

[1] Ubaldi M., Zunino P., Campora U., Ghiglione A., "Detailed velocity and turbulence measurements of the profile boundary layer in a large scale turbine cascade", ASME Paper No. 96-GT-42, 1996.

[2] S. Lardeau, M.A. Leschziner, Li N., "Modelling Bypass Transition with Low-Reynolds-Number Nonlinear Eddy-Viscosity Closure", *Flow, Turbulence and Combustion*, Vol. 73, 2004, pp. 49–76.

[3] L. Cutrone, P. De Palma, G. Pascazio, M. Napolitano, "Assessment of Laminar-Turbulent Transition Models For Turbomachinery Flow Computations", ASME Paper No. GT2005-68330.

[4] Menter F.R., Langtry R.B., Likki S.R., Suzen Y.B., Huang P.G., and Völker S., "A Correlation-Based Transition Model Using Local Variables—Part I: Model Formulation" *J. Turbomach*., Vol. 128, 2006, pp. 413-422.

[5] Sieverding C.H., Cicatelli G., Desse J.M., Meinke M., Zunino P., *Experimental and Numerical Investigation of Time Varying Wakes behind Turbine Blades,* Vieweg, Braunschweig, 1999.

[6] Cebeci T., Smith A.M.O., *Analysis of Turbulent Boundary Layers*, Academic Press, New York, 1974.

[7] Bellhouse B. J., Schultz, D. L., Determination of mean and dynamic skin friction, separation and transition in low-speed flow with a thin-film heated element, *J. Fluid Mech..,* Vol. 24, 2, 1966, pp. 379-400.

[8] Pucher P., Göhl R., Experimental Investigation of Boundary Layer Separation With Heated Thin-Film Sensors, *J. Turbomach*., Vol. 109, 1987, pp. 303-309.

[9] Halstead D. E., et al., Boundary Layer Development in Axial Compressors and Turbines-Part 1 of 4: Composite Picture, ASME Paper No. 95-GT-461, 1995.

[10] Hodson H.P., Boundary-Layer Transition and Separation Near the Leading Edge of a High-Speed Turbine Blade, *ASME J. Eng. Gas Turbines Power*, Vol. 107, 1985, pp. 127-134.

[11] Campora U., Pittaluga F., Ubaldi M., Zunino P., A Detailed Investigation of the Transitional Boundary Layer on the Suction Side of a Turbine Blade, *XV Symposium on Measuring Techniques in Transonic and Supersonic Flow in Cascades and Turbomachines*, Firenze, 2000.

[12] White F.M., *Viscous Fluid Flow*, McGraw-Hill, Singapore, 1991.

[13] Romano G.P., "The Measurements of Structure Functions with Laser Doppler Anemometry", *Ninth International Symposium on Application of Laser Anemometry to Fluid Dynamics*, Lisbon, 1998.